Reducing the influence of STI on SONOS memory through optimizing added boron implantation technology

Xu Yue(徐跃)[1, 2, †], Yan Feng(闫锋)[2], Li Zhiguo(李志国)[3], Yang Fan(杨帆)[3], Wang Yonggang(王永刚)[3], and Chang Jianguang(常建光)[3]

(1 College of Electronic Science & Engineering, Nanjing University of Posts and Telecommunications, Nanjing 210003, China)
(2 College of Electronic Science & Engineering, Nanjing University, Nanjing 210093, China)
(3 Semiconductor Manufacturing International (Shanghai) Corporation, Shanghai 201203, China)

Abstract: The influence of shallow trench isolation (STI) on a 90 nm polysilicon–oxide–nitride–oxide–silicon structure non-volatile memory has been studied based on experiments. It has been found that the performance of edge memory cells adjacent to STI deteriorates remarkably. The compressive stress and boron segregation induced by STI are thought to be the main causes of this problem. In order to mitigate the STI impact, an added boron implantation in the STI region is developed as a new solution. Four kinds of boron implantation experiments have been implemented to evaluate the impact of STI on edge cells, respectively. The experimental results show that the performance of edge cells can be greatly improved through optimizing added boron implantation technology.

Key words: shallow trench isolation; compressive stress; boron segregation; added boron implantation
DOI: 10.1088/1674-4926/31/9/094003 **EEACC:** 2570

1. Introduction

At present, shallow trench isolation (STI) has been broadly used in deep sub-micron VLSI processes for isolation purposes. However, as the scaling down of CMOS device continues, STI has a non-negligible influence on device performance[1−3]. It has been reported that there are mainly two kinds of influence coming from STI[4−8]. One important impact is STI mechanical stress, which is generated at the STI/Si interface and generally shows compressive stress in nature[4]. STI stress could extend into the active area (AA) nearly 300–350 nm and reach several hundreds mega Pa[4]. The main cause of inducing STI mechanical stress is thermal mismatch stress. This originates from the thermal expansion coefficient discrepancy between silicon and STI[4, 5]. The STI-induced stress magnitude depends on the width of STI wells and AA for a given process. A larger STI width or a narrower AA width will generate more mechanical stress in the AA corner[5]. The other important STI impact is boron segregation, namely, boron atoms at the AA edge surrounded by STI could diffuse out to STI, which will decrease the boron concentration at the Si/SiO_2 interface[6−8]. If the AA width becomes narrow enough, the effect of boron segregation along STI corners will further reduce the boron concentration even at the center of the device channel, and its influence will depend on the AA width. The impacted distance of boron segregation can reach about 100 nm[8]. Thus, for those devices with an AA width below 100 nm, boron segregation will play a major role in the formation of boron concentration that must be correctly addressed.

Although many efforts have been made to reduce the STI impact and enhance MOSFET device performance[1, 5], the STI influence on non-volatile memories (NVMs) has been barely studied. With CMOS technology scaling down sub 90 nm, the STI influence on NVM cells becomes much more serious. In this paper, we have mainly investigated the impact of STI on a polysilicon–oxide–nitride–oxide–silicon (SONOS) type NVM a 90 nm localized charge-trapping memory (NROM™). In the experiments, we have found that edge memory cells adjacent to STI have different threshold voltage (V_{th}) distributions and longer ready-busy (RB) programming times as compared to center memory cells. Further, the compressive stress and boron segregation induced by STI are considered as the main causes of these problems. Finally, an added boron implantation in the STI region near the AA edge as a new solution has been presented to reduce the STI-induced impact. Several different added boron implantation experiments were implemented to evaluate the improvement in the performance of edge cells, respectively.

2. Experimental results and discussion

NROM™ is a representative localized charge-trapping non-volatile memory that can store two separate physical bits per cell[9]. The NROM storage layer consists of cladding oxide layers and a nitride layer, forming an oxide–nitride–oxide (ONO) stack[9]. Programming was performed by channel hot electron (CHE) injection into the nitride layer[10], and erasing was performed by band-to-band-generated tunnel-assisted hot-hole injection (HHI)[11]. Read was performed by interchanging the role of the source and the drain. The NROM array architecture is a symmetric high-density virtual ground array, as demonstrated in Fig. 1. The array consists of a cross stack of perpendicular bit lines (BLs) and horizontal word lines (WLs). Here, BLs are embedded N^+ diffusion stripes and WLs are polysilicon stripes. As seen in Fig. 1, only edge cells are adjacent to STI relative to center cells. Thus, the NROM array structure is very suitable for studying the impact of STI on

† Corresponding author. Email: xuyue_cd@163.com
Received 18 February 2010, revised manuscript received 30 April 2010

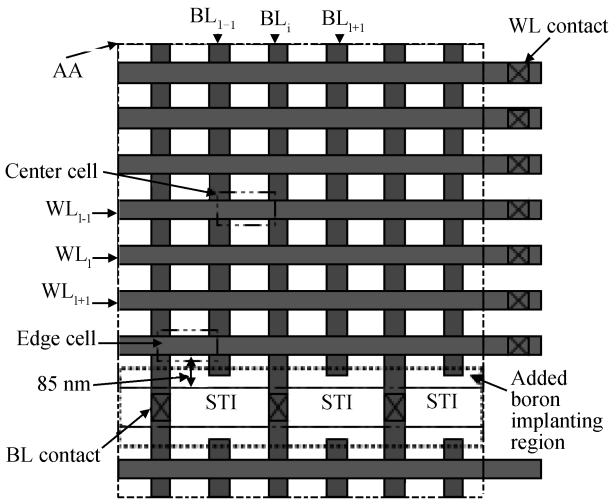

Fig. 1. NROM array schematic diagram in the experiments.

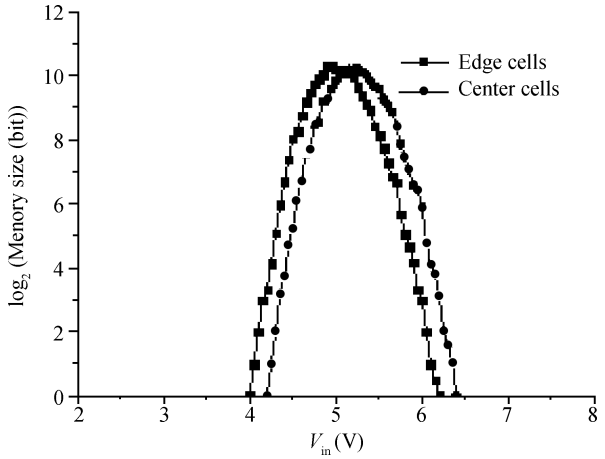

Fig. 2. Initial V_t distribution of edge and center cells on the page level.

NVM through a performance comparison between edge and center cells. In the experiments, both WL width and spacing are designed to be 90 nm. BL width and the channel length are designed to be 100 nm. The distance from the edge WL to the STI corner is designed to be 85 nm, which could decide the magnitude of STI impact.

In this study, the V_{th} distribution of edge and center cells was examined on the array level using the Personal Kalos 2 test system. Figure 2 illustrates the initial V_{th} distribution of NROM cells which are not programmed or erased. There are two curves for one page center cells and one page edge cells respectively, with 32 kbits in each page. We can clearly find that the initial V_{th} distribution of edge cells is inconsistent with that of center cells. The edge cells show a slightly lower initial V_{th} distribution than the center cells.

In addition, RB time, corresponding to the overall programming time per page, was monitored to study the CHE programming behaviors of edge and center cells on the array level using the Personal Kalos 2 test system. When one cell is programmed, the BL (drain) applies about a 5 V pulse and the other BL (source) is grounded. The WL (gate) is forced at about a 9 V pulse and the substrate is grounded. Then CHE injection

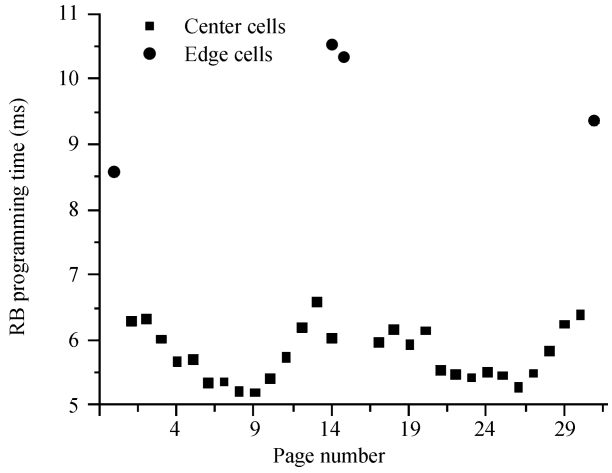

Fig. 3. RB programming time of 32 page cells.

will generate near the drain side. As a result, the V_{th} of the drain side increases. Figure 3 shows the RB time of 32 page cells. In these pages, pages 0, 15, 16 and 31 are edge cells, and the rest of the pages are center cells. It is evident in Fig. 3 that edge cells need about twice as long an RB time than center cells. The average RB time per page for center cells is about 5800 μs, while that rises to about 9.75 ms for edge cells. The longer RB time indicates the lower CHE programming efficiency of edge cells under the same bias voltage.

The experimental results show that the performance of edge cells deteriorates compared with center cells, indicating that edge cells may suffer from a serious STI influence. In fact, compressive stress and boron segregation induced by STI should be responsible for these problems. The low programming efficiency of edge cells resulting from boron segregation can be explained as follows. When the CHE injection mechanism is applied, an electron must have enough kinetic energy over 3.15 eV to surmount the tunnel oxide barrier and inject into the storage layer. The channel electrons are accelerated from the source side to the drain side under positive drain bias and reach their maximum kinetic energy when arriving in the drain region, and hence CHE injection always happens near the drain side. During the acceleration, the electrons will encounter optical phonon scattering and lose their kinetic energy[12]. Boron segregation leads to a lower concentration in the channel region of edge cells, which will result in a lower local electric field at drain side under the same drain bias. As a result, fewer "lucky" electrons can avoid the scattering and acquire enough kinetic energy to inject into the storage layer in a short time. Therefore, edge cells need a longer RB programming time to reach the same V_{th} shift in comparison with center cells, which is in good agreement with the experimental result illustrated in Fig. 3.

For the problem of non-uniform V_{th} distribution between edge and center cells, STI compressive stress and boron segregation together should answer for it. It is known that STI compressive stress could reduce electron mobility[1, 5], which will lead to an increase in V_{th} of edge cells. On the other hand, boron segregation will lead to a decrease in V_{th} of edge cells due to the lower boron concentration in the channel region. If the edge cells suffer a greater influence from boron segrega-

Table 1. Four kind of added boron implantation conditions.

Technology	Tilt (°)	Energy (keV)	Dose (cm^{-2})	Element
A	0	20	5×10^{12}	^{11}B
B	0	30	5×10^{12}	BF_2
C	10	20	1×10^{13}	^{11}B
D	10	30	1×10^{13}	^{11}B

tion, they will have slightly lower initial V_{th} distribution than the center cells. This situation has been well confirmed by the experimental result shown in Fig. 2.

In order to reduce the influence of STI, an added boron implantation in the STI BL contact region as a new solution is put forward. The added boron implantation region is shown in Fig. 1. The distance from the boron implantation region to the two adjacent edge WLs is 35 nm. Added boron implantation could locally increase the boron concentration in the edge channel region so that the CHE programming efficiency of edge cells could be improved. At the same time, the V_{th} distribution difference between the edge and center cells could also be reduced due to an increase in V_{th} of edge cells.

3. Several different implantation technologies

Four kinds of added boron implantation technologies were carried out to investigate the impact of STI on edge cells. The technology conditions are shown in Table 1. Technology A is a vertical implantation with 20 keV energy and 5×10^{12} cm^{-2} dose. Technology B is also vertical implantation with the same implantation dose, but the implantation energy is 30 keV. Both technologies C and D apply 10° tilted implantation with 1×10^{13} cm^{-2} dose. The implantation energy is 20 keV in technology C and 30 keV in technology D. The implantation of BF_2 is selected in technology B, and ^{11}B is chosen in the rest of the technologies.

After each added boron implantation, the V_{th} distribution width (VDW) and RB time of 32 page cells, including 28 page center cells and 4 page edge cells, were tested to evaluate the improvement in the performance of edge cells. The VDW is equal to the maximum V_{th} minus the minimum V_{th}. Figure 4 shows the average initial VDW per page. To get a convenient comparison, the results of the "skip" technology without added boron implantation is also shown in Fig. 4. It can be seen that there only exist small VDW differences between edge and center cells after applying technologies A, B and D. However, a distinct VDW difference can be observed in technology C. Here, the VDW of center cells is 2.0 V, but that of edge cells reaches about 2.5 V. Further, taking all the edge and center cells into consideration, the overall VDW was also measured, illustrated in Fig. 4. The greater deviation between the overall VDW and the center VDW indicates the greater non-uniformity of V_{th} distribution between the edge and center cells. We can observe that there is a maximum deviation value of 1 V in technology C. A deviation value of 0.85 V exists in technology D. Only a deviation value of 0.55 V occurs in technologies A and B, as compared with 0.6 V in the "skip" technology. Consequently, the V_{th} distribution difference between edge and center cells can be slightly reduced in technologies A and B, but this difference is increased in technologies C and D, with a particularly great rise in technology C.

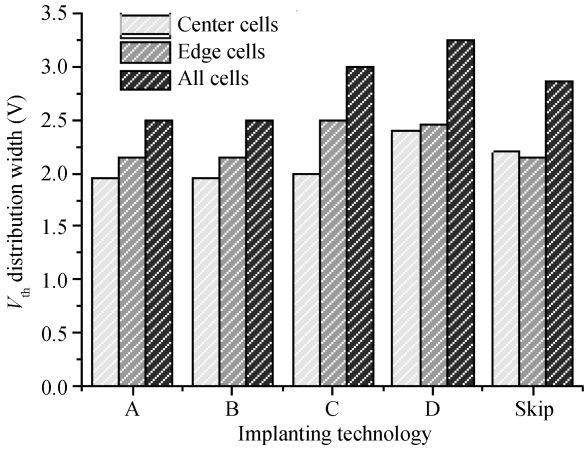

Fig. 4. Initial V_{th} distribution width after added boron implantation.

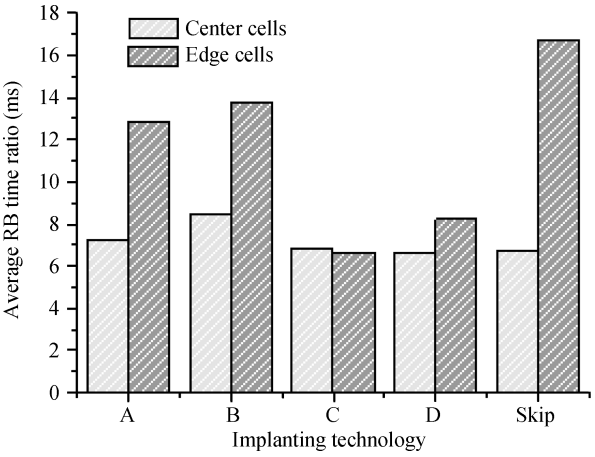

Fig. 5. Average RB time after added boron implantation.

Figure 5 shows the average RB time per page after the four kinds of added boron implantation. It is evident that the RB time of edge cells in technologies C and D has decreased remarkably, and especially in technology C, edge cells exhibit the almost same RB time as center cells. Therefore, the CHE programming efficiency of edge cells can be greatly improved in technologies C and D. The RB time of edge cells has also reduced in technologies A and B, but the reduction is much lower than that in technologies C and D.

Figure 6 shows the relation between average RB time ratio and average VDW ratio for different process conditions. The plane horizontal coordinate presents the ratio of overall VDW to center VDW. The plane vertical coordinate presents the ratio of average RB time of edge cells to that of center cells. As seen in Fig. 6, we can clearly compare the improved performance for edge cells under different implantation processes. Vertical boron implantation in technologies A and B can produce a decreasing V_{th} distribution difference between edge and center cells, but the improvement in programming efficiency is obviously lower than that of the 10° tilted implantation in technologies C and D. Compared with ^{11}B used in technology A, BF_2 implantation in technology B can produce a better edge programming performance with the same VDW. In contrast, 10° tilted boron implantation in technologies C and D can achieve a higher programming efficiency, but the V_{th} distribu-

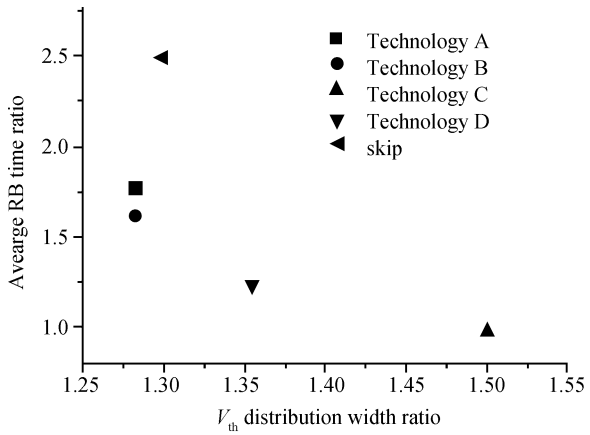

Fig. 6. Average RB time ratio versus V_{th} distribution width ratio.

tion difference between edge and center cells becomes larger. In technology C in particular, edge cells obtain the maximum programming efficiency, but it is impossible for this to be accepted by actual application due to the large non-uniformity of V_{th} distribution. By comparison of the experimental results, technology D should be the optimizing process, because it can produce an acceptable V_{th} distribution difference and achieve a high programming efficiency for edge cells simultaneously.

The experimental results suggest that the STI influence on edge cells can be remarkably reduced through optimizing the added boron implantation conditions. Compared to vertical boron implantation in technologies A and B, it is more effective in increasing the boron concentration at the AA edge for 10° tilted implantation in technologies C and D. So, the CHE programming efficiency of edge cells in technologies C and D has been improved remarkably. Although processes C and D use the same implantation dose, the edge channel region has the higher boron concentration in technology C due to the smaller implantation energy. As a result, edge cells in technology C have obtained a higher CHE programming efficiency. As the higher doping concentration induces a larger decrease in electron mobility in technology C, edge cells exhibit a larger V_{th} distribution inconsistency compared with center cells. However, the appropriate implantation dose and energy in technology D give the edge cells a high programming efficiency and an acceptable V_{th} distribution difference. Because of relatively low boron concentration of edge cells in technologies A and B, the improvement in the programming efficiency of edge cells is less obvious than that in technologies C and D. But the V_{th} distribution inconsistency between edge and center cells shows a slight decrease due to the reducing influence of boron segregation in technologies A and B. Compared to ^{11}B implantation in technology A, BF_2 implantation in technology B makes it easier to form a shallow junction. Thus, the edge channel region in technology B has a slightly higher boron concentration so that edge cells obtain a slightly higher CHE programming efficiency.

4. Conclusion

In this paper, a SONOS type memory has been used to study STI-induced impact on memory cells. It has been found that edge cells adjacent to STI have a lower programming efficiency and a different V_{th} distribution compared with center cells. The compressive stress and boron segregation induced by STI are considered to be the main reasons for these problems. Finally, we develop an added boron implantation in the STI region as a new solution to mitigate the impact of STI. Four kinds of added implantation technologies were implemented to analyze the improvement in the performance of edge cells. The experimental results have proved that the performance of edge cells can be remarkably improved through optimizing the added boron implantation conditions.

References

[1] Miyamoto M, Ohta H, Kumagai Y. Impact of reducing STI-induced stress on layout dependence of MOSFET characteristics. IEEE Trans Electron Devices, 2004, 51(3): 440

[2] Callon C, Reimbold G, Ghibaudo G, et al. Electrical analysis of mechanical stress induced by STI in short MOSFETs using externally applied stress. IEEE Trans Electron Devices, 2004, 51(8): 1254

[3] Sheu Y M, Yang S J, Wang C C, et al. Modeling mechanical stress effect on dopant diffusion in scaled MOSFETs. IEEE Trans Electron Devices, 2005, 52(1): 30

[4] Moroz V, Eneman G, Verheyen P, et al. The impact of layout on stress-enhanced transistor performance. International Conference on Simulation of Semiconductor Processes and Device, 2005: 143

[5] Kahng A B, Sharma P, Topaloglu R O. Exploiting STI stress for performance. IEEE Conference on Computer–Aided Design, 2007: 83

[6] Machala C, Wise R, Mercer D, et al. The role of boron segregation and transient enhanced diffusion on reverse short channel effect. IEEE International Conference on Simulation of Semiconductor Processes and Devices, 1997: 141

[7] Kuo P, Hoyt J L, Gibbons J F. Effects of strain on boron diffusion in Si and SiGe. Appl Phys Lett, 1995, 66(5): 580

[8] Ghetti A, Benvenuti A, Molteni G, et al. Experimental and simulation study of boron segregation and diffusion during gate oxidation and spike annealing. IEDM Tech Dig, 2004: 983

[9] Eitan B, Pavan P, Bloom I. NROM: a novel localized trapping, 2-bit nonvolatile memory cell. IEEE Electron Device Lett, 2000, 21(11): 543

[10] Lusky E, Shacham-Diamand Y. Investigation of channel hot electron injection by localized charge-trapping nonvolatile memory devices. IEEE Trans Electron Devices, 2004, 51(3): 444

[11] Larcher L, Pavan P, Eitan B. On the physical mechanism of the NROM memory erase. IEEE Trans Electron Devices, 2004, 51(10): 1593

[12] Pavan P, Bez R, Olivo P, et al. Flash memory cells—an overview. Proc IEEE, 1997, 85(8): 1248